ERROR MODELLING ON REGISTRATION OF HIGH-RESOLUTION SATELLITE IMAGES AND VECTOR DATA

Pu-Huai Chen [a] *, Szu-Chi Hsu [a], Ge-Wen Lee [b]

[a] Dept. of Surveying and Mapping Eng., Chung-Cheng Institute of Technology, Ta-Hsi, Taoyuan, 335 Taiwan, R.O.C.
phchen@ccit.edu.tw
[b] Dept. of Civil Eng., Chung-Cheng Institute of Technology, Ta-Hsi, Taoyuan, 335 Taiwan, R.O.C.

Commission I, WG I/4

KEY WORDS: Geometric, Integration, Matching, Raster, Registration, Structure, Understanding, Vector

ABSTRACT:

Traditionally, image-and-map registration is carried out using low-level image processing techniques. One of inevitable problems resulted from a low-level image processing technique is the need to decide what the ultimately desired object is. An alternative way to register images and maps is to use a 'top-down' or high-level image understanding approach, for instance, a geometric-structure-matching (GSM) technique. The algorithm of the proposed GSM technique is validated using a Quickbird image and the corresponding cadastral map. The boundary lines and polygons of cadastral parcels are used as the elements of geometric structure in the studied case. An automatic technique has been developed to match image features and the corresponding vector data. In addition, prior knowledge about the error model in the procedures of image-and-map matching has not been fully understood, therefore, this paper also concentrates on the error model required to implement the algorithm and to achieve a high level of automation. The error model is vital to give a threshold for optimising the results of the proposed GSM technique. Preliminary results show that errors of the order of 5m from the procedures of image-and-map registration are possible, and that error is comparable with the predicted one. It is possible to eliminate the requirements of manual intervention for registering images and maps, provided that accurate vector data are available. Potential applications of the proposed algorithm include providing ground control for automatic photogrammetry and updating data of spatial information systems.

1. INTRODUCTION

High-resolution images taken by advanced sensors with ground sampling distance (GSD) on the order of less than 1m, such as Quickbird and Ikonos data, keep flowing in, and users of various fields demand reasonable solutions from photogrammetry and remote sensing community to cope with the needs of map revision and extraction of information promptly. Automation is always the main consideration for solving the above-mentioned requests. Many efforts have been made to understand and to extract information from images, and this kind of photogrammetric approaches can be called as forward solutions or 'bottom-up' approach. Unfortunately, the current methods for automatic extraction of information from satellite images are still far from practical. In general, the reason why visual brains of human beings are able to draw a map by using complex images is rather poorly understood, if not entirely unknown. This explains why the development of algorithms for automatic extraction of spatial information is progressing slowly (Sowmya and Trinder, 2001).

On the contrary, currently available data, such as vector data, maps, and digital elevation models (DEMs), representing basic knowledge about areas of interest, have been proved useful for providing information of ground control for map revision and photogrammetric, or radargrammetric, tasks (Morgado and Dowman, 1997; Chen and Dowman, 2000; Habib and Kelley, 2001). Comparing with traditional photogrammetric approach, this kind of operations might be called as reverse solutions or 'top-down' approach. Automatic image-and-map registration is still one of unsolved problems in pursuit of fully automatic photogrammetry, near-real-time map revision and smart spatial information systems (Dowman, 1998; Heipke *et. al*., 2000). Traditionally, image-and-map registration is carried out using low-level image processing, or 'bottom-up', techniques. One of inevitable problems resulted from low-level image processing techniques is the need to decide what the ultimately desired object is. Since that the decision is made by a human operator after segmentation of features, obviously, the need of human interventions in the traditional processing procedures results in relatively low level of automation. An alternative way to register images and maps is to use a 'top-down' or high-level image understanding approach, provided that prior knowledge about image-and-map registration is available and applicable in automatic procedures (Shapiro and Stockman, 2001; Baltsavias, 2004).

There is no intention in the paper to give a precise definition of knowledge, however, prior knowledge is referred to as any geo-spatial data or models available, such as roads, boundary lines and land parcels, which give geometric structure of areas of interest. Hence, the paper is aimed at using geometric structure defined by vector data, given by existing 2-D maps or spatial information systems, for image-and-map registration with a higher level of

* Corresponding author.

automation. Cadastral parcels surrounded by wall features are of particular interest in the paper, and research is being focused on the analysis of the geometric characteristics of walls and land parcels. It should be noticed that prior knowledge about the error model in the procedures of image-and-map matching has not been fully understood. An error model is vital to give reasonable thresholds for optimising the automatic procedures of the proposed GSM technique.

In Section 2, an error model is proposed not only to implement the algorithm in order to achieve high level of automation, but also to provide a sound theoretic basis for error evaluation of the proposed algorithms. The algorithm of the proposed GSM technique is validated using a sub-scene of standard Quickbird image and the corresponding cadastral map given by the relevant authority, as described in Section 3. An analysis is done using manual image-and-map registration in Section 3 to be compared with the automatic approach in Section 4. Automatic techniques have been developed and tested to match image features and the corresponding vector data, as shown in Section 4. Brief discussion and conclusions are covered in Section 5.

2. THEORY

2.1 Basis of Image-and-Map Registration

The basic requirements of image-and-map registration include well-defined co-ordinate systems and identifiable features for image and map space. On the one hand, spatial information systems provide specific layers of vector data (polygons) over areas of interest in co-ordinate system of selected map projection. The landscape of areas of interest can change following local development or construction works, however, most of the cadastral parcels remain unchanged. On the other hand, the cadastral parcels characterized by boundary lines, such as walls, provide features found in high-resolution optical images taken by space-borne advanced sensors, as shown in Fig.1.

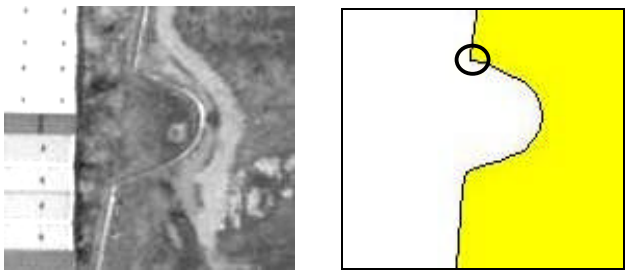

(©Quickbird Image Copyright 2002, Digital Globe)

Figure 1. (Left) A patch (165 lines by 182 pixels) of Quickbird standard image at Taoyuan, Taiwan. (Right) A segment of a cadastral map provided by the Government of Taoyuan County, Taiwan. The circled node shows a wall feature.

Since that walls are observable features appearing in high resolution satellite images or on air photos and are approximate boundary lines of cadastral parcels, therefore, it is straightforward to utilize geometric structure defined by lines/polygons to register map and image, leading to the proposal of a geometric-structure-matching technique in this paper.

2.2 Basis of Geometric-Structure-Matching

'Structure' can mean relational structure or semantic structure as the terms used by the pattern recognition and computer vision community (Shapiro and Haralick, 1981; Wang, 1998), however, it is referred to as the geometric structure in this paper. Roughly speaking, the so-called geometric structure can be given by the co-ordinates of nodes of each polygon, or endpoints of each line. A cadastral parcel given by governmental spatial information systems is defined by numerous nodes with known ground co-ordinates, which give an exact geometric structure that can be employed to guide the search of wall features in image space, provided that wall features are detectable and applicable. It is observed that wall features in satellite images show an U-shape intensity profile normal to the bearings of walls as shown in Fig.2. The bottom of U-shape curve corresponds to the shadow of a wall illuminated by the sun.

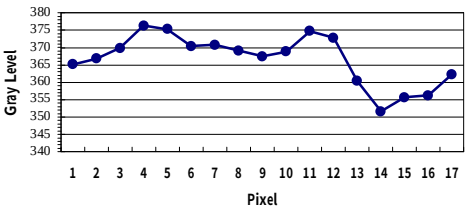

Figure 2. An intensity profile normal to the bearing of a wall.

In order to detect wall features in high-resolution satellite images, the height of wall and the sun azimuth/angle data provided by image header data have to be introduced to form a wall model in image space. The width of the shadow of walls of height h under solar illumination of solar altitude θ is derived as $s = h\cot\theta$ on the ground. Given that h=2m and θ =72 °, the shadow of the wall exhibits a dark line of width 0.65m, or 1~2 pixels, in a vertical satellite image. In case of oblique photography with tilt angle Ω, the wall itself can be observed and be projected onto image space, showing a bright line of width w given by $w = h\cot\Omega$. Thus, a dark-and-bright line pair exhibits a wall observed in an oblique high-resolution satellite image, giving a U-shape model of an intensity profile. In automatic approach, each polygon has to be employed to search across the boundary lines, pixel by pixel, to find and record candidate locations regarding to the U-shape model of intensity profile. The extent to be searched is determined by an error model, to be established in next section.

For constructing a correct U-shape model of each polygon along the wall feature, the length between the contiguous nodes in the polygon is used as the first weighting factor to reduce the effects resulted from obscured features, assuming that a long wall feature always keeps the same radiometric characteristics along the boundary line. Since

the shadow of a wall is changeable, according to the bearings of wall features α_w and the solar azimuth α_s, thus, the second weighting factor to be considered is given by

$$\begin{aligned}
&\cos(\pi/2-|\alpha_s-\alpha_w|), \text{ if } 0\le|\alpha_s-\alpha_w|<\pi/2\\
&\cos(|\alpha_s-\alpha_w|-\pi/2), \text{ if } \pi/2\le|\alpha_s-\alpha_w|<\pi\\
&\cos(3\pi/2-|\alpha_s-\alpha_w|), \text{ if } \pi\le|\alpha_s-\alpha_w|<3\pi/2\\
&\cos(|\alpha_s-\alpha_w|-3\pi/2), \text{ if } 3\pi/2\le|\alpha_s-\alpha_w|<2\pi
\end{aligned} \quad (1)$$

In order to carry out image-and-map registration, the vector data of the cadastral parcels with walls have to be provided by spatial information systems and then converted into image space, according to the imaging geometry and/or the processed level. If the header data of Quickbird images gives relatively good approximate geographic location of each corner, say on the order of 10m, it is possible to start image-and-map registration with no human intervention at all. However, selecting a reference point manually identifiable both on map and in image could speed up registration. The U-shape model of intensity profile of a shaded wall is certainly not secured to find an unique location for image-and-map registration, therefore, the geometric characteristics of all polygons, i.e., all of the given parcels with walls, have to be taken into account. Then, all of the searching results of polygons are compared with each other to filter out any candidate locations whose geometric structure is not conformal to the vector data. In other words, most of the polygons should have the best match at the candidate locations with the same magnitude of translation and rotation.

2.3 Image-and-Map Registration Error Modelling

Automation of photogrammetric practices are mainly based upon prior knowledge derived from the manual operations, therefore, error modelling on image-and-map registration has to start with the analysis of the errors resulted from manual operations. In case of the registration of a vector map and a geometrically rectified image, the errors of registration may result from various aspects. Errors coming from a rectified image include residuals of rectification σ_r, random errors in co-ordinate measurements of features/points σ_m and misplacements of the identified features σ_f, such as walls, with respect to the expected boundary lines. On the other hand, errors resulted from a vector map contain residuals of surveying adjustment σ_s and the error of digitisation of cadastral maps σ_d. Obviously, image-and-map registration is a process of linear combination of two types of data, and the resultant error σ_o is propagated and derived as

$$\sigma_o=\sqrt{\sigma_r^2+\sigma_m^2+\sigma_f^2+\sigma_s^2+\sigma_d^2} \quad (2)$$

The magnitude of rectification error σ_r depends upon the imaging geometry, algorithms of rectification, ground control/DEMs, and the terrestrial flatness. Since the advanced satellite optical sensor produces images of 0.6m GSD, it is not always available to derive DEMs of excellent accuracies on the order of deci-meter, and the production of ortho-rectified high-resolution satellite imagery of good quality is not guaranteed. However, the rectification of satellite images over flat areas does not necessarily need DEMs, and the proposed algorithm for image-and-map registration is primarily aimed at flat areas at this stage. Ground control is also not essential, provided that on-board satellite positioning systems gives good approximation of geographic locations for images. Thus, the imaging geometry of the satellite sensor and the algorithm to be used in rectification has to be considered. Assuming that the rotational angles in across-track direction (pitch) and in vertical direction (yaw) are relatively small and neglected, the first author proposes a simplified equation to calculate the relief displacement d_t resulted from undulated terrain surface in oblique satellite images regarding to the rotational angles in along-track direction (roll). It is given as

$$\begin{aligned}
&\text{if } H\gg h, \text{ then } d_t\approx h\frac{(f-r\tan t)(f\tan t+r)}{Hf(1+\tan^2 t)};\\
&\text{if } t\to 0, \quad \text{then } d_t\approx h\frac{(f-0)(0+r)}{Hf(1+0)}=h\frac{r}{H}
\end{aligned} \quad (3)$$

where H= flying height, h=difference of elevation, f= focal length, t= tilt angle (roll), r=radial distance from center to an arbitrary point in image space. It can be calculated that an elevation difference of 10m over the entire imaging area may result in difference of relief displacement less than 0.3 pixels, in the case of the Quickbird imagery. This modest displacement is due to the imaging geometry of extremely narrow angular filed of view and relatively flat terrain. Since the cadastral parcels are located at relatively flat areas, where terrain variations are under 10m, the magnitude of rectification error σ_r is relatively insignificant.

The second factor of errors σ_m is caused by random errors in co-ordinate measurements of features/points and is related with the image sampling and re-sampling procedures. It is obvious that a line feature of ground distance of 1 GSD in a basic (raw) image taken (sampled) by a satellite sensor may be sampled by 2 pixels in a standard image, i.e., the blurred edges of the line features in a rectified and re-sampled (standard) image convey deviations up to 2 pixels. The third factor of errors σ_f is due to intentional misplacements of the identified features, such as walls, in respect to the expected boundary lines. Regulations of local governments demand some extent of retreat in setting up walls regarding to the exact boundary lines of a cadastral parcel to give way to the surrounding roads and sidewalks. The extent of the retreat of wall is up to 3 m, or 5 pixels in Quickbird imagery, contributing the major error to the results of image-and-map registration. The forth factor of errors is the residuals of cadastral surveying and adjustment σ_s conveyed in the vector data of cadastral parcels. The residuals of cadastral surveying practices and adjustment computations are on the order of centimetres, which is certainly much better than one GSD of any advanced satellite optical sensor available. That is also the reason why cadastral maps are proposed to provide ground control for image-and-map registration.

In case that digitization for existing cadastral maps, instead of surveying by using total-station or electronic distance measurement (EDM) instruments, are the sources of vector data, the fifth factor of errors σ_d is resulted from the process of digitization. The scale of cadastral maps is 1/500 (urban areas) or 1/1,000 (rural areas) for the new version of cadastral maps in Taiwan and is 1/600 (urban areas) or

1/1,200 (rural areas) for the old version. The new version of cadastral maps in Taiwan is reliable and is employed in this paper. It is estimated that an error, resulted from the precision of digitizers and the process in digitization, up to 0.3 mm is possible, which leads to an error of 15~30cm as a result. Obviously, the error of digitisation of cadastral maps is still less than one pixel in Quickbird imagery. To sum up, the error model based upon equation (2) and the above inference gives an error of 6 pixels due to various causes. The error model also implicitly indicates that using wall features for the registration of Quickbird images and vector data is liable to result in errors up to 6 pixels or 4.2m.

3. TEST DATA

3.1 Test Image and Cadastral Map

A sub-scene of a panchromatic standard (rectified) Quickbird image taken on 26th May, in 2002, in Taoyuan County, Taiwan, covering an area of 2.5×1.6 km^2, as shown in Fig.3, where undulation of terrain surface is under 5m in the test area, is to be registered with a cadastral map conveying several parcels with wall features, as shown in Fig.4.

(©Quickbird Original Image Copyright 2002, Digital Globe)

Figure 3. A sub-scene of Quickbird standard image over Taoyuan, Taiwan. Size:2.5×1.6 km^2.

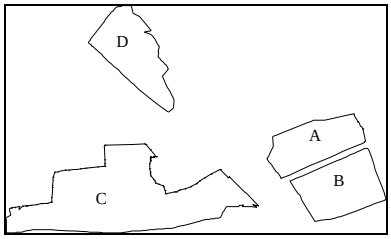

(Courtesy by Taoyuan County Government, Taiwan, ROC)

Figure 4. Four polygons extracted from a cadastral map, to be registered with the satellite image.

The geometric consistency of the standard image can be validated using a two-dimensional conformal (four-parameter) transformation, which describes the geometric conformation between the two sets of co-ordinates in terms of their geometric relationship, such as a scaling factor, a rotational angle and two translations, for GPS-measured ground points and manually measured co-ordinates on the satellite image. The header data of a satellite image gives a scale of the image pixel to actual ground distance, and the co-ordinates of the image points are recorded and transformed into a local co-ordinate system. Since the extent of the test areas is relatively small, Datum shifts are of no concern in validating the test images. Table 1 gives the results of geometric inconsistency check on the two sets of measured co-ordinates. The geometric inconsistency or the precision of rectification of the test image, in terms of 6 GPS-measured points between two sets of co-ordinates derived by using four parameters transformation, shows that the root of mean squared error (RMSE) of the 6 points is approximately 2 pixels (σ_r = 2 pixels), as demonstrated in section 2.3. This is obviously owing to a relatively flat terrain surface in the test areas.

6 GPS-measured points	RMSE	Mean	Max.	Min.	Extent
Easting	1.6	0	+2.1	-2.3	4.4
Northing	1.2	0	+1.1	-1.4	2.5
Error Vector Length	2.0	(Unit: pixels)			

Table 1. The evaluation of the geometric consistency of the sub-scene Quickbird standard image.

3.2 Manual Image-and-Map Registration

Automation is aimed at replacing the role of human operators in some sorts of process or systems. Thus, human knowledge about the principles of the photogrammetric processes is essential for the evaluation of the desired automatic process. In order to validate the proposed error model, 22 'control features' (nodes of polygons of cadastral parcels) are selected manually from the test image and vector map. Among those points ('control features'), 8 points are used as GCPs in a projective transformation between the test image and the vector map, and the other 14 points as check points. The best estimations of the parameters of each transformation function are derived using a least squares adjustment procedure, and these parameters formulate a transformation function allowing the other 14 points to be transformed and compared. Figure 5 shows the residual error vectors of 8 GCPs using a projective transformation between the co-ordinates manually measured in image and on a vector map, respectively. The results summarized as in Table 2 show the accuracies of 14 check points using a projective transformation between the co-ordinates measured in the test image and on the vector map. Figure 6 demonstrates the distribution of the resultant errors of the check points, showig that there is no systematic error. The RMS errors shown in Table 2 give magnitudes of the resultant errors derived from the process of manual image-and-map registration and are comparable with the theoretical error predicted in Section 2.

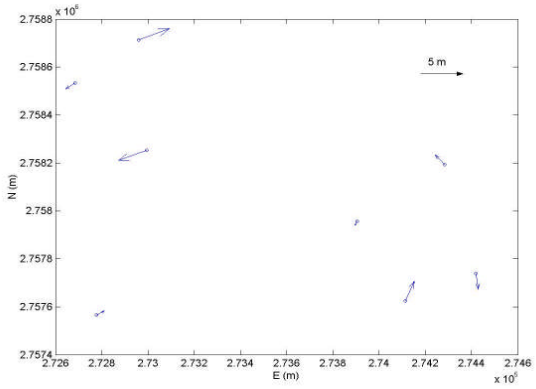

Figure 5. The residual error vectors of 8 GCPs using a projective transformation between the co-ordinates manually measured in image and on a vector map, respectively.

19 Check points	RMSE	Mean	Max	Min	Extent
Easting	3.2	-1.1	4.8	-6.5	11.3
Northing	3.1	1.9	6.3	-2.5	8.5
Error Vector Length	4.5	(unit: m; 1m=1.4 pixel)			

Table 2. The accuracies of the 14 check points using a projective transformation between the co-ordinates manually measured in image and on a vector map, respectively.

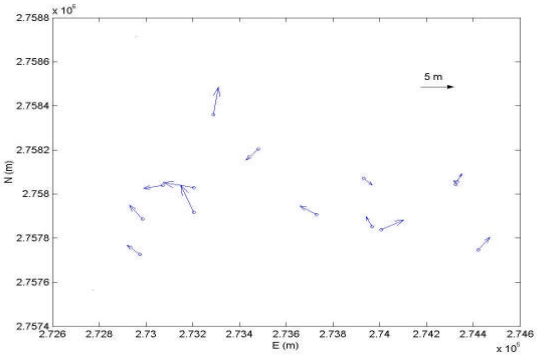

Figure 6. The residual error vectors of check points.

4. AUTOMATIC IMAGE-AND-MAP REGISTRATION

The automatic procedures of the image-and-map registration start from an initial location of an arbitrarily selected reference points in the test image and the corresponding node on the vector map. A reference point of good approximation is not essential for the proposed algorithm for image-and-map registration, but it does reduce the time required to carry out image-and-map registration. The Quickbird image header data provide useful information of map projection (UTM) and co-ordinates of four corners, giving relatively close approximation with deviations of translation on the order of less than 100m. In addition, rotational errors are not significant in this case, since the provided information of map projection of image co-ordinates gives enough knowledge for datum transformation between the local datum of the vector map and that of the rectified satellite imagery. Since the proposed model of the line feature is sensitive to noise in the matching procedure, a huge amount of candidate locations can be produced by the image-and-map registration. Thus, the critical procedure in the image-and-map registration is to find the best match of the line features of both types of data using the proposed geometric-structure-matching algorithm. The primary results as shown in Table 3 suggests that a large portion of the population of candidate locations can be eliminated up to 98% without using any other criteria for the image-and-map registration. In Table 3, the searching range is defined as the extent or the number of pixels in respect to the reference point.

All of the polygons are registered according to the same geometric structure as mentioned before, however, each polygon needs to be registered individually in the first place. Further refining processes for the remaining candidate locations are required in order to pick up the best estimation of registration, which is done by an analysis of the density numbers for the linear features. Since the linear features always convey similar radiometric characteristics, such as homogeneous density numbers along a specific linear feature or boundary line, it is proposed that the variances of density numbers of all pixels along a specific linear feature, such as a wall feature, have a minimal difference.

Searching range (in pixel)	Candidate locations of each polygon				Geometric-structure-matched candidates
	A	B	C	D	
20	502	453	509	557	36
40	1826	2031	1382	1563	178
100	14188	13913	11192	14166	1096
200	57572	57651	47637	55710	4692

Table 3. The number of candidate locations of the primary image-and-map registration using the geometric-structure-matching technique.

(©Quickbird Original Image Copyright 2002, Digital Globe)

Figure 7. The result derived using the geometric-structure-matching technique for automatic registration of a Quickbird image and a cadastral map.

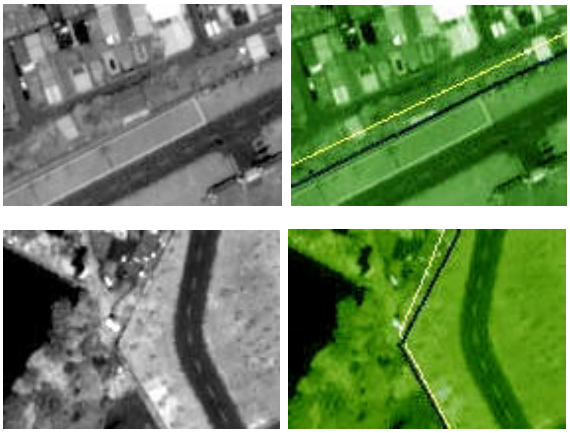

(©Quickbird Original Image Copyright 2002, Digital Globe)

Figure 8. A patch of the Quickbird image shows the result of image-and-map registration. Left: the original images. Right: the boundary lines of parcel are colored as yellow and the blue color lines denote wall features.

The primitive result derived using the geometric-structure-matching technique for automatic registration of a sub-scene of Quickbird imagery and a cadastral map is as shown in Figure 7. The four bright polygons represent cadastral parcels. A patch of the satellite image over the test area is shown as in Fig. 8, with the wall feature (blue lines) and the corresponding boundary line (yellow lines). Further work on improving the automatic algorithm and the relevant evaluation on the results of the image-and-map registration is in progress.

5. CONCLUSIONS

The algorithm of the proposed GSM technique has been validated using the Quickbird image and the corresponding cadastral map. The boundary lines and polygons of cadastral parcels are used as the elements of geometric structure in the studied case. Automatic techniques have been developed to match image features and the corresponding vector data. An error model in the procedures of image-and-map matching has been proposed. The error model is required to implement the algorithm of image-and-map registration in order to achieve high level of automation. The error model provides a threshold for optimising the results of the proposed GSM technique. The experimental results show that the magnitude of the error on the order of 4.5m resulted from the image-and-map registration algorithm is possible, and those errors are comparable with the predicted ones (4.2m). It is possible to eliminate the requirements of manual intervention for registering images and maps, provided that accurate vector data and header data of satellite images are available. Further work on improving the automatic algorithm and the relevant evaluation on the results of the image-and-map registration is in progress. Potential applications of the proposed algorithm include providing ground control for fully automatic photogrammetry and updating data of spatial information systems.

ACKNOWLEDGEMENTS

The result presented in this paper is part of the work in the project NSC 92-2211-E-014-006 sponsored by the National Science Council, ROC. The satellite image presented in the paper is sponsored under the project NSC 91-2211-E-014-007. The authors are grateful to the Government of Taoyuan County, Taiwan, ROC, for providing a digital map of cadastral parcels. The authors are also in debt to Professor C.-C. Chang and his group and Dr. S.-A. Chen for giving help on GPS field work and computational adjustment for the GPS observations.

REFERENCES

Baltsavias, E.P., 2004. Digital ortho-images — a powerful tool for the extraction of spatial and geo-information. *ISPRS J. of Photogrammetry & Remote Sensing*, 51, pp.63-77.

Chen, P.-H. and Dowman, I., 2000. Geocoding using stereo-generated DEMs and automatically generated GCPs. *International Archives of Photogrammetry and Remote Sensing*, Amsterdam, Netherlands, Vol.33, Part B1, pp. 38-45.

Chen, P.-H. and Dowman, I., 2001. A weighted least squares solution for space intersection of spaceborne stereo SAR data. *IEEE Trans. on Geo-Science and Remote Sensing*, GE-39(2), pp. 233-240.

Dowman, I., 1998. Automating Image Registration and Absolute Orientation: Solution and Problems. *Photogrammetric Record*, 16, pp. 5-18.

Habib, A. and Kelley, D., 2001. Single-photo resection using the modified Hough Transformation. *Photogrammetric Engineering & Remote Sensing*, 67(8), pp. 909-914.

Heipke, C., Pakzad, K. and Straub, B.-M., 2000. Image Analysis for GIS Data Acquisition. *Photogrammetric Record*, 16(96), pp. 963-985.

Morgado, A. and Dowman, I., 1997. A procedure for automatic absolute orientation using aerial photographs and a map. *ISPRS J. of Photogrammetry & Remote Sensing*, 52(4), pp. 169-182.

Shapiro, L.G. and Haralick, R.M., 1981. Structure description and inexact matching. *IEEE Trans. on Pattern Analysis and Machine Intelligence*, 3, pp. 504-519.

Shapiro, L.G. and Stockman, G., 2001. *Computer Vision*. Prentice Hall, Inc., 580 pages.

Sowmya, A. and Trinder, J., 2001. Modelling and representation issues in automated feature extraction from aerial and satellite images, *ISPRS J. of Photogrammetry & Remote Sensing*, 55, pp. 34-47.

Wang Y., 1998. Principle and applications of structural image matching. *ISPRS Journal of Photogrammetry & Remote Sensing*, 53, pp. 154-165.